Added value of advanced methods for seismic verification of existing vertical cylindrical liquid storage tanks and their foundations

F. Besseling MSc
Team leader Earthquake engineering & Structural dynamics at Witteveen+Bos

M. Versluis MSc
Structural engineer Hydraulic structures at Witteveen+Bos

A. Bougioukos MSc
Structural engineer Earthquake engineering & Structural dynamics at Witteveen+Bos

Hydrodynamic pressures

When a liquid storage structure is dynamically excited, hydrodynamic pressures occur on walls, bottom and possibly on the roof. This first has been elaborated for dams by Westergaard [1]. Later, i.a. Housner [2] has developed similar solutions for (rigid) liquid storage tanks in which a distinction is made between impulsive and convective pressures. i.a. Veletsos and Yang [3] have introduced a third term which takes into account the flexibility of the structure. These three terms of the total (horizontal) hydrodynamic pressure are explained in equation (1).

In the these expressions a cylindrical coordinate system (r,z,θ) is used with the origin at the centre of the tank bottom and the positive z-axis in the direction of the fluid.

Rigid and flexible impulsive pressures

The impulsive pressure is the result of the fluid mass which moves with the container wall. A distinction is made between the mass that moves with the ground acceleration (rigid) and the mass that moves with the acceleration difference between ground and wall acceleration (flexible). The rigid impulsive pressure distribution has the shape of a parabola, the flexible impulsive pressure distribution depends on the mode shapes of the structure. Figure 1 shows normalized impulsive pressure distributions calculated with equation (2) which can be found in EN 1998-4 and [3].

In case of a rigid tank (ψ(z) = 1), the expression for the flexible impulsive pressure will result in the expressions for rigid impulsive pressure.

For liquid storage containers the ratio H/R (fluid height / radius) is the most important geometrical parameter that determines the seismic load level. This is because the opposing walls influence each other. In the case of navigation locks and dams it can be shown that when the chamber or reservoir length is more than 4 times the water depth, the pressure is independent of the geometry besides the water depth [1,6].

$$p_{h,dyn}(\xi,\varsigma,\theta,t) = p_i(\xi,\varsigma,\theta,t) + p_c(\xi,\varsigma,\theta,t) + p_f(\xi,\varsigma,\theta,t) \quad (1)$$

In which:

$p_i(\xi,\varsigma,\theta,t)$ = rigid impulsive pressure component
$p_c(\xi,\varsigma,\theta,t)$ = convective pressure component
$p_f(\xi,\varsigma,\theta,t)$ = flexible impulsive pressure component

$$p_i(\xi,\varsigma,\theta,t) = C_i(\xi,\varsigma)\rho H cos(\theta) A_g(t)$$
$$p_f(\xi,\varsigma,\theta,t) = C_f(\xi,\varsigma)\rho H cos(\theta) A_f(t) \quad (2)$$

In which:

$$C_i = 2\sum_{n=0}^{\infty} \frac{(-1)^n}{I_1'(v_n\gamma^{-1})v_n^2}\cos(v_n\varsigma) I_1(v_n\gamma^{-1}\xi);\ C_f = 2C\sum_{m=1}^{\infty}\frac{\delta_m}{v_m}\varepsilon_m\cos(v_m\varsigma)$$

$$v_n = \frac{2n+1}{2}\pi;\ v_m = \frac{2m-1}{2}\pi;\ \delta_m = \frac{1}{H}\int_0^H \psi(z)cos(v_m\varsigma)dz\,;\ \varepsilon_m = \frac{I_1[v_m\gamma^{-1}]}{I_1'[v_m\gamma^{-1}]};\ ;$$

$$C = \frac{\int_0^{H_s}\mu_s(z)\psi(z)dz + m_r\psi(H_s) + 2m\gamma\sum_{m=1}^{\infty}\frac{(-1)^{m+1}}{v_m^2}\delta_m\varepsilon_m}{\int_0^{H_s}\mu_s(z)\psi^2(z)dz + m_r\psi^2(H_s) + 2m\gamma\sum_{m=1}^{\infty}\frac{\delta_m^2\varepsilon_m}{v_m}}$$

$$\xi = \frac{r}{R};\varsigma = \frac{z}{H};\gamma = \frac{H}{R}$$

A_g = horizontal base acceleration; A_f = horizontal acceleration of wall relative to base
H = fluid height; H_s = shell height; R = tank radius; ρ = fluid density; m_r = roof mass;
ψ = mode shape in vertical direction; μ_s = shell mass per unit of height; m = total fluid mass
I_1 = 1st order modified Bessel function

$$p_c(\xi,\varsigma,\theta,t) = C_c(\xi,\varsigma)\rho cos(\theta) A_{cn}(t) \quad (3)$$

In which:

$$C_c = 2R\sum_{n=1}^{\infty}\frac{\cosh(\lambda_n\gamma\varsigma)J_1(\lambda_n\xi)}{(\lambda_n^2-1)\cosh(\lambda_n\gamma)J_1(\lambda_n)}$$

A_{cn} = acceleration for convective mode n
J_1 = 1st order Bessel function; λ_n = roots of 1st derivative of 1st order Bessel function:
$\lambda_1 = 1.8412; \lambda_2 = 5.3314; \lambda_3 = 8.5363; \lambda_4 = 11.7060; \lambda_5 = 14.8636$; etc.

Convective pressures

The convective pressure results from the sloshing of the fluid in standing waves. Figure 2 shows the pressure distribution over the height of the container which is calculated according to equation (3).

Because the fundamental eigen-period of the convective mass is in most cases for ground-supported structures much larger than the fun-

Abstract

Earthquakes cause (hydro)dynamic actions on (steel) liquid storage tanks. In static conditions the tank shell of a vertical cylindrical liquid storage tank is mainly subjected to circumferential (ring) forces. Earthquake excitation results an additional horizontal load component to the tank structure, disturbing the axi-symmetric stress state. This can cause damage if tanks are not properly designed for this specific type of load. Designs of new to be built tanks are often easily adjusted at some specific aspects in order to increase seismic resistance. Typically, simplified design codes that cover these important structural aspects are used for design. More advanced verification/design analysis specifically have significant added value for existing storage tanks not designed to resist seismic loads or for design optimizations in general. This paper focuses on these advanced seismic verification methods and relates them to the behaviour of tanks under seismic response and relevant failure mechanisms. In addition this paper focuses on specific issues that are relevant in relation to seismic design of tank foundations and liquefaction hazard and soil-structure interaction effects. Special focus is put on the shortcomings and limitations of simplified methods and the benefits that more advanced additional verifications can have for clients that develop or exploit tank storage facilities.

Figure 1 *- Horizontal impulsive pressure distributions on tank wall for H/R = 0.8 and θ = 0*

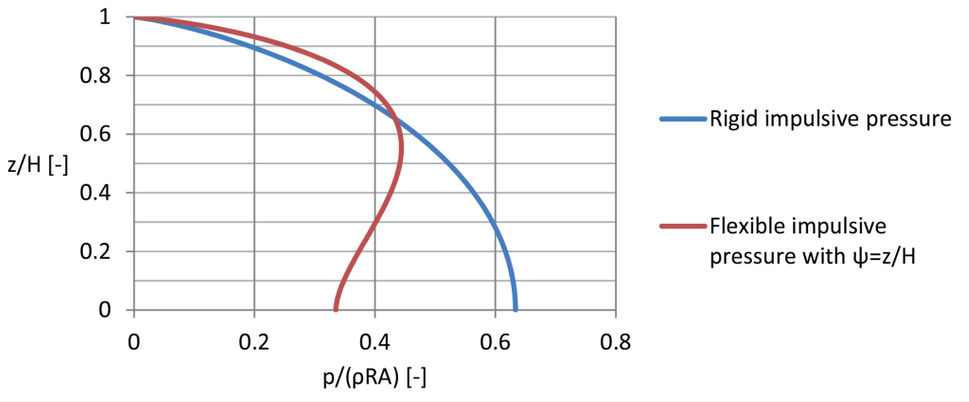

Figure 2 *- Convective impulsive pressure distributions on tank wall for H/R = 0.8 and θ = 0*

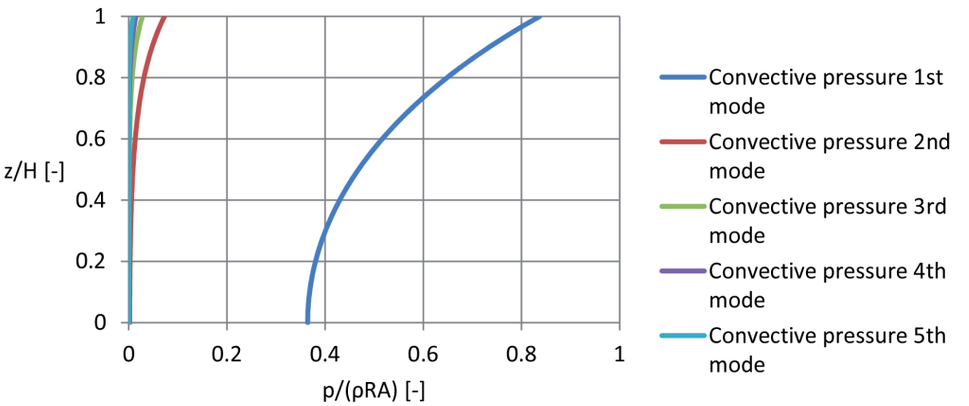

damental eigen-period of the impulsive mass, dynamic coupling between the modes can be neglected. In literature the convective pressure is therefore calculated based on the geometry (H/R) and independent of the flexibility of the fluid container. In case of elevated tanks the fundamental periods can be much closer to each other and dynamic coupling can only be disregarded if the fundamental periods are at least a factor 2.5 separated [7]. For ground-supported tanks of common H/R ratios the convective pressure contributions from higher order modes are negligible and can be sufficed with considering only the fundamental convective mode. The eigen-periods follow equation 4.

$$T_{cn} = \frac{2\pi}{\sqrt{g\frac{\lambda_n}{R}tanh(\lambda_n\gamma)}} \qquad (4)$$

The compressibility of the fluid can also result in hydrodynamic pressures, but this is mainly relevant for high head dams and not for liquid storage tanks of common dimensions [1,6]. The resultant of the hydrodynamic pressure on the walls and tank bottom causes an overturning moment and a base shear.

It is important to realize that the vertical excitation of the earthquake also causes hydrodynamic pressures. Although these are axi-symmetric (and therefore do not result in an overturning moment), they cause an increase/decrease of the total internal pressure. Because the internal pressures influences the buckling resistance in steel tanks, the vertical excitation direction should be included in the analysis.

Failure mechanisms

The following sections describe some of the most critical failure modes observed for liquid storage tanks subjected to earthquake motions. It is not intended to provide a complete list of possible failure modes here. Instead, we address some failure modes of specific interest in relation to analysis methods described in other sections of this paper.

Overturning

In case of horizontal earthquake excitation, mass inertia of the tank structure and the liquid product of hydrodynamic pressures result in global overturning. Anchored and unanchored tanks can be distinguished. For anchored tanks specific anchor elements mount the tank superstructure to the foundation. These anchors should be designed to resist overturning action. For unanchored tanks overturning stability is provided by the weight of the fluid on the bottom plate and more specifically on the annular ring. This annular ring is a strengthened ring plate that should have sufficient width to accommodate plastic rotations and limit uplift of the tank. Post earthquake observations of tank failures in some cases shown poor performance for tanks without a properly designed or constructed annular ring configuration. Moreover, meridional (axial) compression stresses at the compressed side of unanchored tanks increase in case of uplift at the tension side. This should be accounted for in the design.

Figure 3 - *Typical buckling modes of tank*

a) Elastic local buckling due to Livermore earthquake, 1979

b) Elastic-plastic local buckling (elephant-foot) due to the San Fernando earthquake, 1971

c) Shear buckling due to Livermore earthquake, 1979

Photo: J. Skogh (a,c) / http://shellbuckling.com/ (a,b,c)

Shell buckling

Overturning moment action results in increasing meridional membrane stresses. Two main dominant failure mechanisms can be observed, namely the elastic shell buckling (diamond shape buckling mode) and the elastic-plastic shell buckling (elephant's foot buckling shape). In addition, in the area of the shell perpendicular to the direction of loading, shear buckling can occur. The three shell buckling modes are illustrated by figure 3.

The internal hydrostatic and hydrodynamic pressures form an important parameter for shell buckling behaviour. Compared to empty tanks, increasing internal fluid pressure initially stabilizes the tank shell. However, with increasing internal pressure at some point the threshold level of allowable meridional stress drops rapidly as the hoop stress reaches the Von Mises yield stress. This is illustrated by figure 4, in which the horizontal axis shows a dimensionless coefficient of internal pressure (hoop stress versus yield stress) and the vertical axis shows the elastic α_{xpe} and elastic-plastic α_{xpp} pressurized reduction factors from EN 1993-1-6.

The same principle holds for shear buckling. Internal pressures stabilizes the shell and when the hoop stress is 30% of the yield stress or larger, shear buckling does not occur [8]. In practice this means that lower shell courses of filled tanks are generally not susceptible to shear buckling tanks.

Annular ring failure

The annular ring forms a strengthened segment of the bottom plate of a tank. Other portions of the bottom plate are typically constructed of steel plates with less thickness and lower weld capacities. Any plastic rotations should concentrate in the annular ring in order to prevent failures due to insufficient rotation capacity of the bottom plate. The width and welding detailing of the annular ring therefore are essential for the seismic resistance of unanchored tanks.

Foundation failure

Seismic foundation failure of storage tanks on shallow pad or plate foundations can relate to overturning resistance, liquefaction effects, or a combination of both. When during a design phase of a tank facility potentially liquefiable deposits are encountered, often piled foundations are constructed or liquefaction mitigation measures are taken during construction (e.g. dynamic compaction or stone columns). However, these measures have high consequences in terms of costs and impact on operations for existing tanks that would need measures to achieve sufficient safety against liquefaction. In this perspective detailed investigation of tank foundation stability in relation to liquefaction is worthwhile.

Figure 4 - *Schematic influence of tensile hoop stress on the meridional buckling stress [9]*

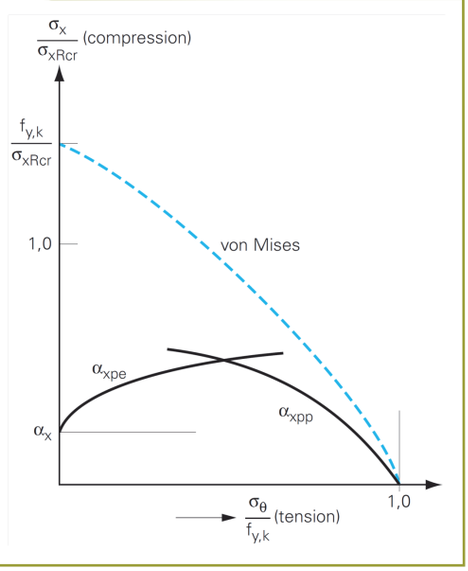

Analysis and design methods

Simplified methods

In Europe, the Eurocodes EN 1993-4-2 and EN 1998-4 are the main standards available for the (seismic) design and verification of liquid storage tanks. Specific rules for design and manufac-

turing of welded steel vertical cylindrical tanks can be found in EN 14015. In addition, buckling of steel shell structures is covered by EN 1993-1-6.

Annex A of EN 1998-4 and annex G of EN 14015 (based on the American API 650) give recommendations and design graphs/tables to calculate the overturning moment and base shear force with a simple, quasi-static approach of a MDOF system. Based on the H/R ratio, the impulsive and convective modal masses, as well as their acting heights, can be calculated. The sum of the impulsive and convective mass is the total fluid mass. The spectral acceleration of these modes follows from the response spectrum ordinates at the calculated periods.

With this simplified method no distinction is made between the rigid and flexible impulsive mass. Instead, it is assumed that all impulsive mass acts rigid (the parabolic shape), but with the spectral acceleration corresponding to the fundamental eigen-period of the combined tank-fluid system instead of the ground acceleration.

For the considered tanks (0,5 < H/R < 1,0), the resulting base shear and overturning moment from this simplified method match quite well with the results obtained with a modal analysis where each of the three hydrodynamic components are summed up. The same conclusion is drawn in [5], which also gives an elaborate explanation about these simplified methods.

There are also drawbacks of these preliminary design methods:

- The simplified methods do not always include the seismic vertically induced pressure, which influences buckling verifications for steel tanks;
- Shear buckling of steel tanks is not discussed;
- Influence of soil-structure interaction is usually not taken into account;
- Although the overall overturning moment may be correct, the flexibility of the tank wall can cause higher pressure at the top shell courses compared to an assumed rigid pressure distribution (as shown in figure 1). Designing the wall thickness of the upper shell courses with respect to earthquakes proportional to the lower shell course thickness and hydrostatic pressure, as mentioned in annex G4.4 of EN 14015, should therefore be treated with caution.

Figure 5 - *Fundamental mode of tank-fluid system*

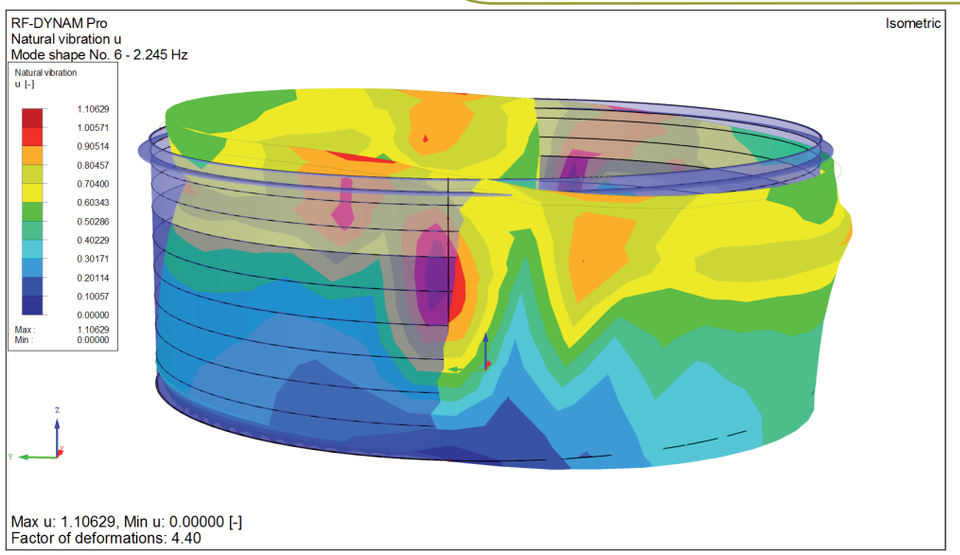

Modal analysis and FSI effects

Besides the simplified method, also a FEM modal analysis can be performed, which can be incorporated in more elaborate evaluation methods like prescribed by EN 1998-4. This part of Eurocode series addresses coupling between hydrodynamic pressure distributions, eigen-periods and mode shapes. Considering FEM modal analysis, two methods can be identified:

- Using added fluid mass in a structural model for eigen-value analysis.
- Using a full fluid-structure interaction (FSI) model for eigen-value analysis.

In the first method the following steps need to be performed:

1. Assume a mode shape for the tank walls;
2. Calculate the added mass distribution according to e.g. Veletsos and Yang [3];
3. Include this added mass with the structural FEM model and perform modal analysis.
4. Extract the mode shape and repeat steps 2 through 4 until convergence is reached.

The above procedure can be performed with most FEM software packages. Figure 5 shows the fundamental mode shape for the tank-fluid system.

The second method approaches the problem by analysing the coupled system of the fluid and the structure; the so-called fluid-structure interaction. The problem is solved through the finite element method in which three types of elements are considered simultaneously; the structure, the fluid and the interface elements. In the structure, the discretization is given in the following form:

$$\mathbf{M}_S\ddot{\mathbf{u}} + \mathbf{C}_S\dot{\mathbf{u}} + \mathbf{K}_S\mathbf{u} + \mathbf{f}_I = \mathbf{f}_S^{ext}(t) \qquad (5)$$

where $\mathbf{M}_S$, $\mathbf{C}_S$, and $\mathbf{K}_S$ are the mass, the damping and the stiffness matrices of the structure respectively, whereas u is the unknown displacement of the structure. The vector f_I represents the interface forces due to interaction between the solid and the fluid, while the vector $\mathbf{f}_S^{ext}$ represents the external load which acts on the structure.

In the case of the fluid, the unknown quantity is the pressure variable p and the interface forces are considered for the coupling with the structure.

At the interface (with the structure) boundary of the fluid the following equation holds:

$$\frac{\partial p}{\partial n} = -\rho_F \mathbf{n}_F^T \ddot{\mathbf{u}}_F \qquad (6)$$

where, ρ_F is the fluid density and $\mathbf{n}_F$ the outward normal to the fluid domain. Considering continuity between the normal displacements of the fluid and the structure with the condition $\ddot{u}_F = \ddot{u}_S$, the last equation (6) becomes:

$$\frac{\partial p}{\partial n} = -\rho_F \mathbf{n}_F^T \ddot{\mathbf{u}}_S \qquad (7)$$

The discretization in the fluid is given in the following form:

$$\mathbf{M}_F\ddot{\mathbf{p}} + \mathbf{C}_F\dot{\mathbf{p}} + \mathbf{K}_F\mathbf{p} + \mathbf{r}_I = 0 \qquad (8)$$

Taking into account that in the element level the

Figure 6 - *left: modelling of fluid-structure interface elements; right: modelling of boundary condition at the surface of the fluid (potential head).*

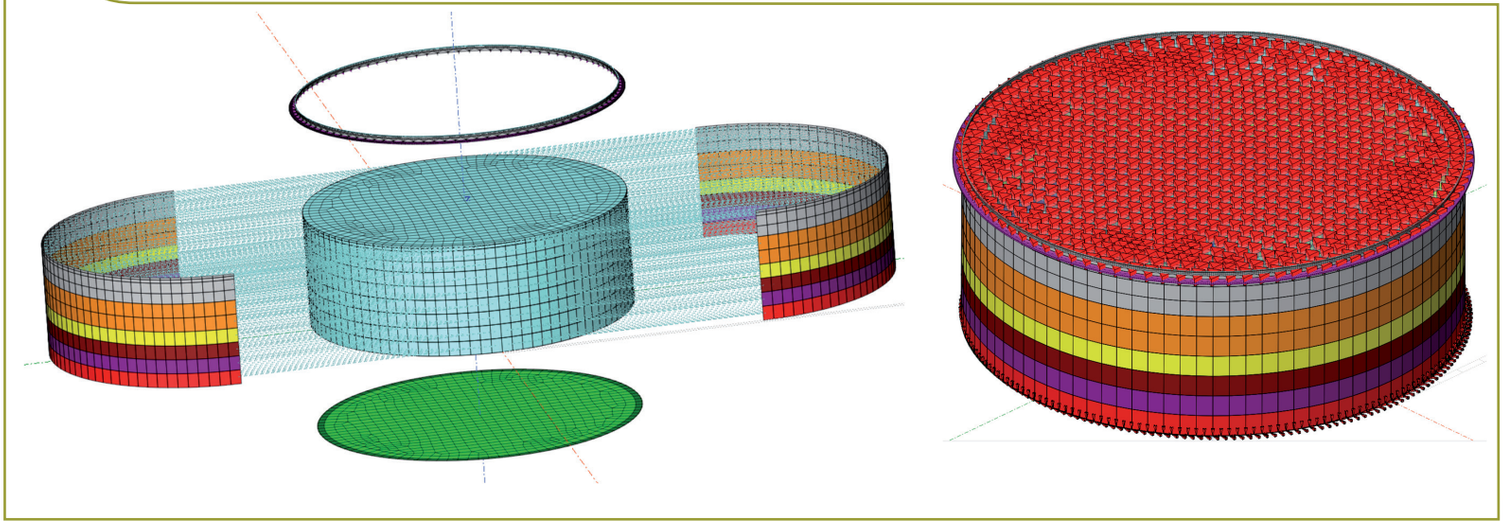

contributions of the interface force is $\mathbf{f}_I^e = -\mathbf{R}^{eT}\,\mathbf{p}^e$ and $\mathbf{r}_I^e = \rho_F\,\mathbf{R}^e\,\ddot{\mathbf{u}}^e$, the coupled system of equations can be obtained:

$$\begin{bmatrix} \mathbf{M}_S & \mathbf{O}^T \\ \rho_F\mathbf{R} & \mathbf{M}_F \end{bmatrix}\begin{Bmatrix} \ddot{\mathbf{u}} \\ \ddot{\mathbf{p}} \end{Bmatrix} + \begin{bmatrix} \mathbf{C}_S & \mathbf{O}^T \\ \mathbf{O} & \mathbf{C}_F \end{bmatrix}\begin{Bmatrix} \dot{\mathbf{u}} \\ \dot{\mathbf{p}} \end{Bmatrix} + \begin{bmatrix} \mathbf{K}_S & -\mathbf{R}^T \\ \mathbf{O} & \mathbf{K}_F \end{bmatrix}\begin{Bmatrix} \mathbf{u} \\ \mathbf{p} \end{Bmatrix} = \begin{Bmatrix} \mathbf{f}_S(t) \\ \mathbf{0} \end{Bmatrix} \quad (9)$$

This system can be solved either in the frequency or in the time domain depending on the type of the external force. Subsequently, an eigenvalue analysis is performed in order to identify the dominant eigen-modes.

Modal analysis and SSI effects

Codes and guidelines for seismic design differentiate two main categories of soil-structure interaction (SSI) effects, being inertial and kinematic interaction. For vertical cylindrical steel storage tanks, inertial interaction is most important. The non-rigid based condition for tanks on shallow foundation introduces an additional degree of freedom in the system which results in an increase of the fundamental period and a potential increase of system damping. The change in system configuration can be visualized by considering the equivalent mechanical spring model of the tank with a rigid foundation on top of an another equivalent mechanical spring-dashpot model of the soil consisting out of translation and rocking springs and dashpots (illustrated by figure 7).

Aiming at correct prediction of period elongation and increased damping the main challenge is to properly quantify the SSI springs and dashpots. Design codes and guidelines typically specify SSI coefficients as function of foundation radius, soil shear modulus and soil Poisson's ratio, with a frequency dependent multiplier [10]. Although this concept may appear quite simple and straightforward, the actual implementation has a few complicating facets. First of all, there may be a scale effect for moderate to large storage tanks on grade. Moreover, rigid slab assumption is not valid for unanchored tanks or tanks on pad foundation which have a relatively flexible bottom configuration. Rigid global rocking behaviour of the tank-foundation pad therefore can be unrealistic. Moreover, the simplified expressions include a single soil shear modulus, for which a constant value is assumed following perfect homogeneous half space conditions. In reality for layered soils shear modulus is not constant and moreover effective shear modulus due to modulus reduction is shear strain dependent and therefore seismic load dependent. The latter implies a non-constant shear modulus over the time frame of an earthquake and a varying effective shear modulus among different zones below and adjacent to the tank.

Figure 7 - *Mechanical model SSI principle.*

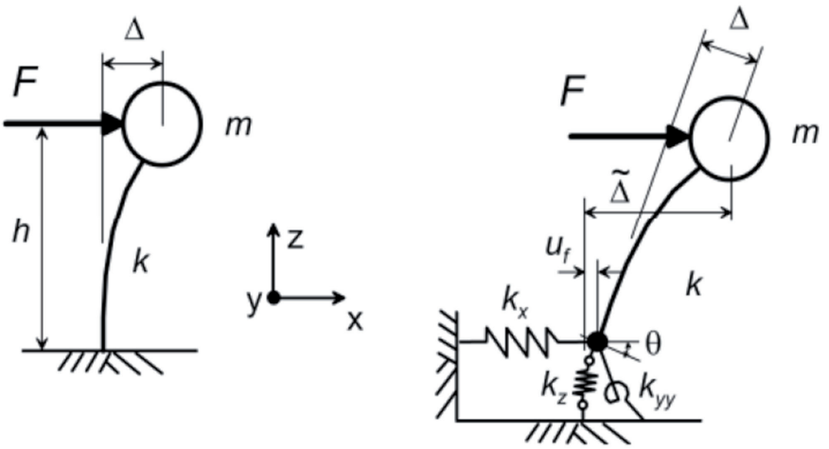

In order to address these issues a combined approach is suggested in which code based expressions supplemented with finite element analysis from the basis of determination of SSI effects. An example for a 60 m diameter tank on layered alluvial deposits is shown below. The first figure illustrates measure shear wave velocity V_s (SCPTU) and correlated (from CPT) V_s and small-strain shear modulus G_0 depth profiles. This information forms the basis for prediction of SSI constants with code based expressions. It can be read that within the influence depth of the tank the effective equivalent small strain shear modulus is approximately 75 MPa in this case.

Figure 8 - *Example of SCPT measured Vs-depth profile and Vs-depth and G0-depth profiles form CPT + correlations*

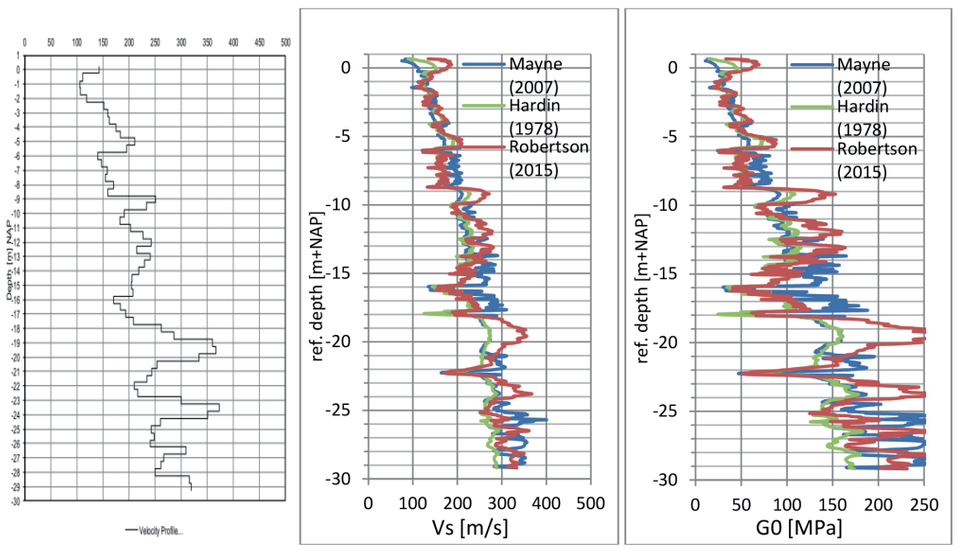

Subsequently, figure 9 shows vertical deformation contours of a tank axi-symmetric model due to a 10% foundation load increase and similarly deformation contours for the tank subject to overturning loading. From these FEM calculations the effective global SSI behaviour can be better understood and static SSI constants can be derived. In this specific case it turned out that the code based formula needed adjusted input values in order to match both horizontal, vertical and rocking response stiffness.

With the reported SSI constants the fundamental period of the system for the specific tank under consideration in this example elongated from approximately 0.37 s to 0.46 s.

Linear bifurcation analysis

In order to determine the local buckling resistance of the shell several types of analyses can be performed, ranging from purely linear analytical expressions (LA stress design) up to full geometrically and physically non-linear analysis with imperfections (GMNIA). Another linear method is the FEM linear bifurcation analysis (LBA), which basically finds the critical Euler buckling force (lowest eigen-value) for the specific shell. In order to find the characteristic buckling stress, the knockdown factor from stress design are applied to the elastic buckling stress from the LBA. These knockdown factors include non-linear effects like imperfections and plasticity. Benefits of a LBA are that the elastic buckling stress of a specific structure can be found, including boundary conditions (e.g. stiffening girders), varying diameter/thickness ratios or asymmetric (hydrodynamic) loading. But also for more standard tanks a higher critical buckling stress can be found compared to the classical expression:

$$\sigma_{x,Rcr} = \frac{Et}{r\sqrt{3(1-\nu^2)}} \approx 0.605E\frac{t}{r} \qquad (10)$$

The eigen-values are dependent of the internal pressure and thus on hydrodynamic loading. Figure 10 shows the first relevant eigen-value for shell buckling for a 60 m diameter tank at a maximum hoop stress of 69% of the yield stress. Based on LBA it was substantiated that the actual critical buckling stress of the specific tank is about 20% higher compared to the basic idealized solutions following from LA stress design.

Pushover analysis

The basic method for performing post-elastic seismic analysis of structural capacity is a non-linear pushover analysis (NLPO). By increasing a load factor on the impulsive load the pushover curve can be calculated. This method can also be used for storage tanks to substantiate the sequencing of the relevant failure modes for a tank. Relevant nonlinearities for unanchored steel vertical cylindrical liquid storage tanks are:

- Foundation overturning and sliding bearing capacities;
- Uplift (compression-only spring supports);
- Plastic material behaviour such that plastic hinges can occur;
- Local buckling of the shell.

One may differentiate ductile mechanism non-linearities from non-ductile (or brittle) mecha-

Figure 9 - *Vertical deformation contours for a tank subject to seismic differential foundation pressures (left: vertical motion; right: is rocking motion)*

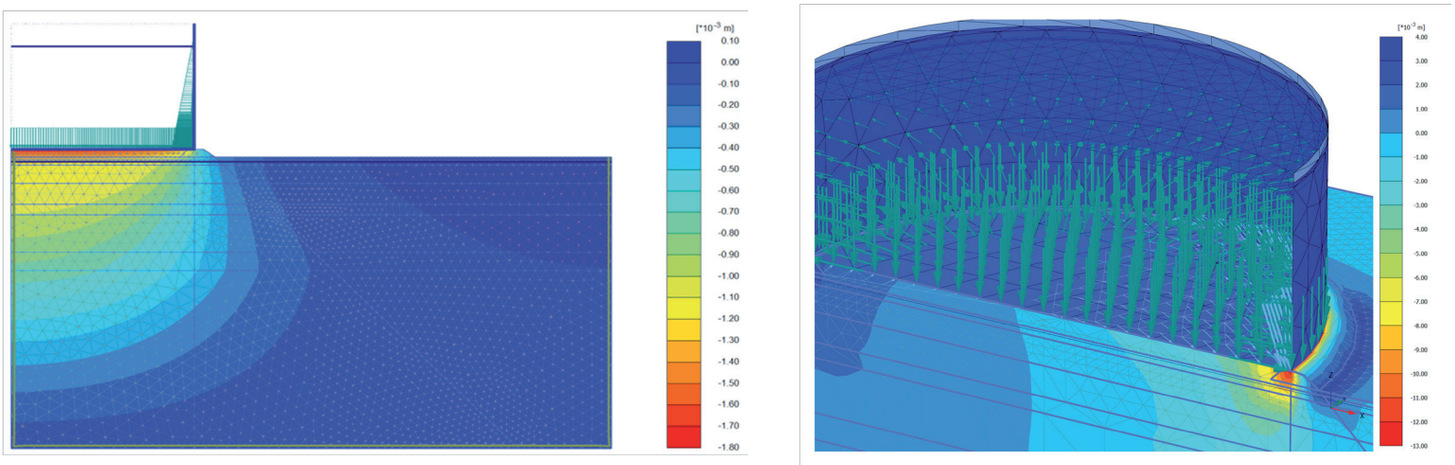

Figure 10 - *Eigen-vector from LBA for a 60 m diameter tank .*

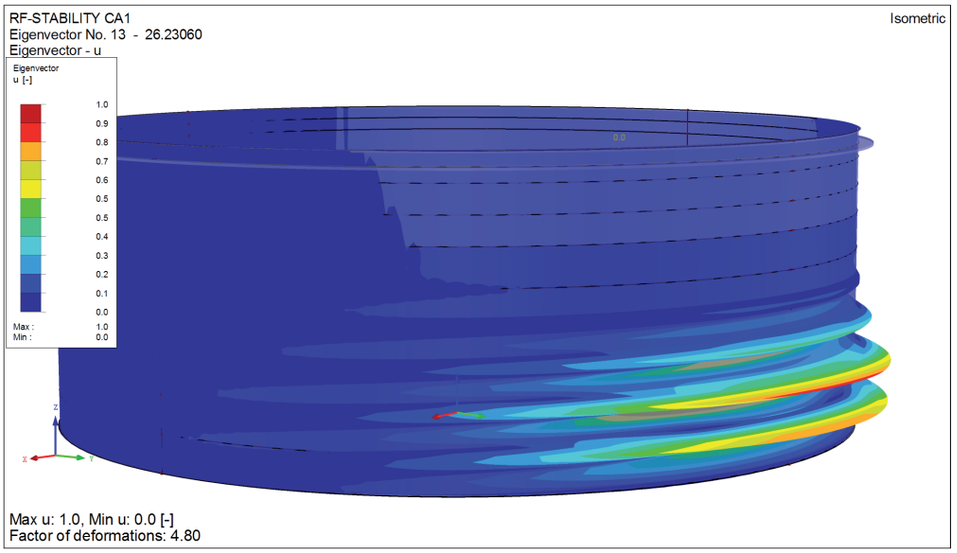

Figure 11 - *Pushover response spectrum analysis result in ADRS format.*

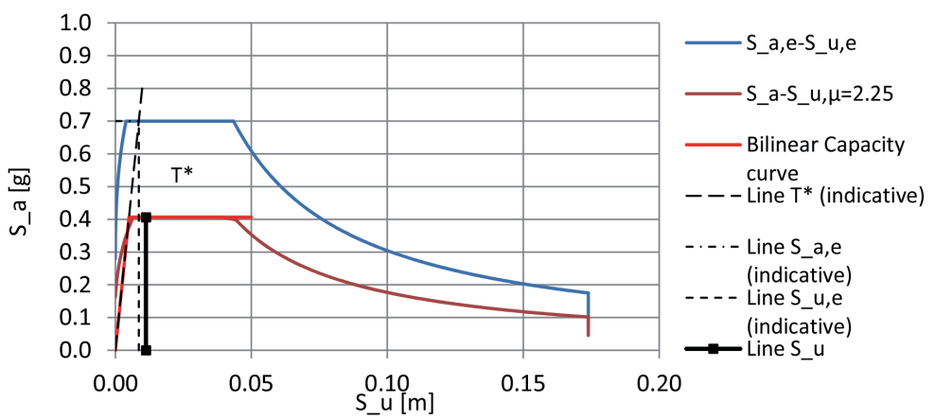

nism nonlinearities. Ductile mechanisms, like uplift and - to some extend - plastic material behaviour, limit the seismic capacity but accommodate nonlinear response can be obeyed to design a tank structure for lower demand spectra. Pushover response spectrum analysis is the tool used for this purpose. As a first step, a nonlinear numerical model of the tank structure is developed. Then a unit load vector representing the impulsive pressure component is calculated. This unit load vector subsequently is applied to the nonlinear numerical model of the tank by gradually increasing its amplitude by scaling the load vector with some scalar. The pushover load range needs to extend well beyond the design seismic demand. The nonlinear pushover curve that is calculated from this analysis then can be coupled in an acceleration-displacement response spectrum (ADRS) framework to the seismic demand and equivalent nonlinear system damping as illustrated by figure 11.

Seismic design of tank foundations

Tank shallow foundations are characterized by large differential stress levels below and next to the tank. As a result, the zone just next to the tank foundation edge shows high initial static shear stress levels in the soil. Depending on the relative density of the soil this can increase or decrease significantly the liquefaction triggering potential of the soil. This is illustrated by figure 12, where on the left hand side shows the static shear stress coefficient for cyclic stress liquefaction triggering analysis according to [11] and on the right hand side shows the impact for a specific tank configuration in terms of calculated excess pore pressure ratio.

A three-step approach is used to evaluate the seismic tank foundation integrity including liquefaction potential. The first step follows from the evaluation of hydrodynamic pressures and global overturning response of the tank, based on which the seismic foundation loads can be calculated. Secondly, empirical methods that predict liquefaction triggering potential predict the level of potential excess pore pressure generation as a function of seismic hazard, ground characteristic and tank configuration (e.g. [11]). In these assessments both effects of increased isotropic stress states below the tank and high shear stress zones next to the tank are accounted for. Then as a final step, a 3D finite element model including tank superstructure, pad foundation and soil stratigraphy is developed. In the layered soil stratigraphy liquefaction effects can be accounted for by explicit modelling of excess pore pressure generation or by means of equivalent reduction of effective friction angle. With this model the (reduced) seismic tank foundation stability can be assessed.

This three-step approach overcomes the need for an effective stress time-dependent finite element model to evaluate liquefaction risks. Although such effective stress models are nowadays rapidly being developed we note here that their implementation currently needs really extensive calibration. One of the reasons for this statement is the impact of initial stress state, which can severely corrupt the numerical performance of such constitutive models [12].

Conclusions and recommendations

The present paper illustrates the added value of integration of simplified and advanced techniques and methods for seismic design/verification of liquid storage tanks. Although simplified code based methods are able to capture the main elements important in seismic response and seismic resistant design, we observe that advanced analysis give much more insight and can be very helpful for improved evaluations. This is of specific interest for tanks not specifically designed for seismic action or tanks in areas subject to changes in seismic code regulations. Integrating advanced techniques in the verification procedure in this case enhances the quality of verifications, gives a more complete assessment of potentially critical elements and helps to optimize the design of any required seismic retrofitting.

References

[1]. Westergaard, H.M., 'Water Pressures on Dams During Earthquakes', Transactions,

American Society of Civil Engineers 98 (1933), nr. 1835, New York (USA), p. 418-472.

[2]. Housner, G.W., 'Earthquake Pressures on Fluid Containers', Eight Technical Report under Office of Naval Research, California Institute of Technology, Pasadena (USA) 1954.

[3]. Veletsos, A.S., Yang, J.Y., 'Dynamics of Fixed-Base Liquid-storage Tanks', Proceedings of U.S.-Japan Seminar on Earthquake Engineering Research with Emphasis on Lifeline Systems, Tokyo (JP) 1976, p. 317-341.

[4]. Scharf, K., 'Beiträge zur Erfassung des Verhaltens von erdbebenerregten, oberirdischen Tankbauwerken', Fortschritt-Berichte VDI, Reihe 4. Bauingenieurwesen, nr. 97 (1990), VDI Verlag, Düsseldorf (D).

[5]. Malhotra, P.K., Wenk, T., Wieland, M., 'Simple Procedure for Seismic Analysis of Liquid- Storage Tanks', Structural Engineering International 10 (2000), nr. 3, p. 197-201(5).

[6]. Versluis, M., (2010), Hydrodynamic pressures on large lock structures, Master thesis TU Delft and Witteveen+Bos, 2010.

[7]. IITK-GSDMA Guideline for Seismic Design of Liquid Storage Tanks - Provisions with Commentary and Explanatory Examples (2007), National Information Center of Earthquake Engineering, Indian Institute of Technology Kanpur.

[8]. Design Recommendation for Storage Tanks and Their Supports With Emphasis on Seismic Design, Architectural Institute of Japan 2010, Tokyo (JP) 2010.

[9]. Rotter, J.M., Schmidt, H., Buckling of Steel Shells - European Design Recommendations, (5th edition), ECCS 125, ECCS, Brussel (BE) 2013.

[10]. Gazetas, G., Analysis of Machine Foundation Vibrations: State-of-the-Art. Soil Dynamics and Earthquake Engineering. 1983, 2(1), 2-43.

[11]. Idriss, I.M., Boulanger, R.W., Soil liquefaction during earthquakes, Monograph EERI MNO-12, Earthquake Engineering Research Institute, 2008.

[12]. Elsäcker, W.A., Evaluation of seismic induced liquefaction and related effects on dynamic behaviour of anchored quay walls - using UBC3D-PLM constitutive model, Master thesis TU Delft and Witteveen+Bos, 2016.

Figure 12 - *Left: example of static shear stress ratio near a tank foundation; right: corresponding concentrating excess pore pressure ratios calculated based on [11]*

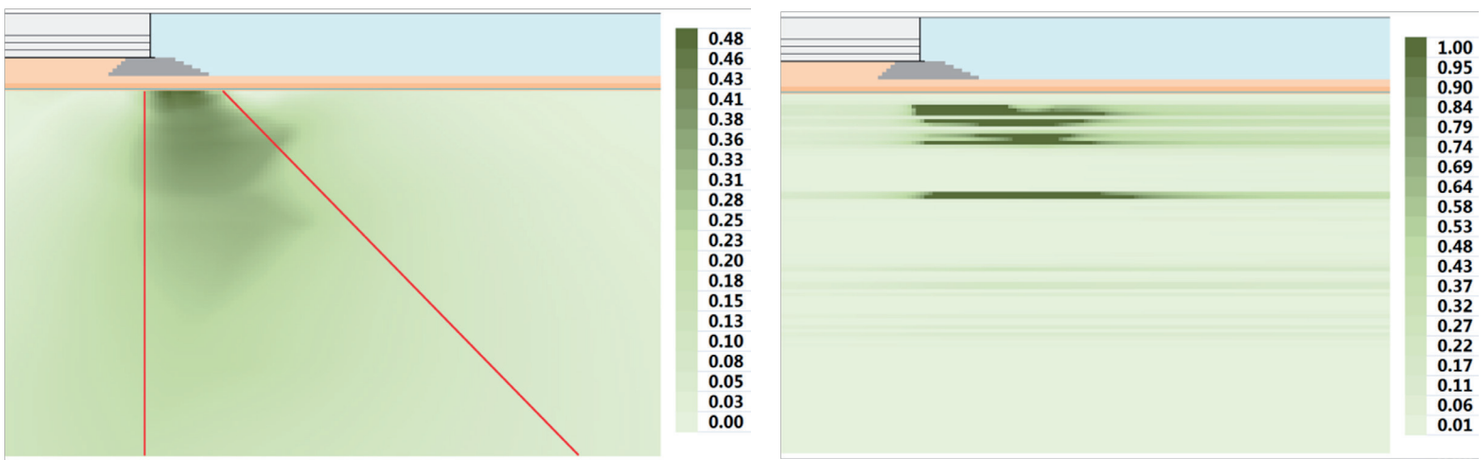

Figure 13 - *Changing foundation failure modes as a result of liquefaction effects (figure shows shear strain contours plots close to failure)*